Tu 2MIN P07

High-Resolution Near-Surface Velocity Model for Depth Imaging of Mineral Deposits in the Ludvika Mining Area, Sweden

L. Schreiter[1]*, S. Buske[1], A. Malehmir[2], E. Bäckström[3], M. Schön[3], P. Marsden[3]

[1] Technical University Of Freiberg, [2] Uppsala University, [3] Nordic Iron Ore AB

Summary

Within the H2020-funded Smart Exploration project existing legacy seismic data acquired in the Ludvika Mines are analysed in order to delineate the deposits in depth. Here we present a velocity model derived using first-break traveltime tomography, which represent the near-surface materials at high resolution and can be directly used for refraction static calculations or incorporation and for depth imaging algorithm. Our results are consistent with derived velocities from downhole logging data and show a strong vertical velocity gradient in the upper first hundred meters. In mineral exploration clear images of the subsurface and an improved characterization of mineral deposits are required to reduce the risk before drilling. Especially in prestack depth imaging workflows, which are successfully applied to hardrock seismic data, a reliable velocity model is required that represents the lateral and vertical variations in lithology and assures the robustness of the velocity model within the application of depth migration routines at the same time. A special focus of this work lies on the derivation of a detailed near-surface velocity model, which accounts for strong scattering effects due to lateral inhomogeneities as well as for topographic effects on the reflections.

Introduction

Within the H2020-funded Smart Exploration project cost-effective and environmentally friendly methods for geophysical exploration are developed in order to improve the depth resolution for different mineral prospecting targets. Innovative methods are developed and tested at different exploration sites to improve resources available and critical for the EU. Our study aims at the characterization of the subsurface and the delineation of mineral deposits at depth. For fulfilling these objectives high resolution three-dimensional images and models are required, which represent the shallow subsurface and enable a validation of their influence on geophysical images of deeper targets. Advanced seismic imaging techniques are proven to reveal clear images in hardrock geological environments, which are characterized by a mainly low signal-to-noise ratio, steeply-dipping structures and strong effects of the near-surface materials. Therefore depth-imaging workflows, which are commonly applied within the oil and gas exploration and rarely used for mineral exploration, require a high-resolution velocity model to compensate the influence of the geological environment on the seismic wavefield. Conventional velocity model building tools, which include the analysis of the reflection moveout while assuming a nearly horizontally layered media, cannot easily be applied for data acquired within a hardrock environment. Consequently we apply a migration velocity model building workflow, which focuses on a detailed representation of the near-surface layer and concurrent assessment of the robustness of the model for later usage within for example focusing seismic imaging techniques, like Fresnel-Volume-Migration (Buske et al., 2009; Hlousek et al., 2015).

In this study, we use a commonly available (to the project partners) legacy data from the Blötberget iron-oxide mining area of Ludvika Mines in central Sweden acquired in two campaigns during 2015 and 2016 (Malehmir et al., 2017; Maries et al., 2017a) for deriving a high resolution near-surface velocity model by a first break traveltime tomographic approach. Results of this work will improve the seismic image quality in depth domain and reduce the risk in future drilling operations.

First-break traveltime tomography

Wide-angle as well as near-vertical surface seismic data are used for the derivation of the velocity model. Different seismic datasets (i.e., 2015 and 2016) are initially treated separately and are integrated in a second step in order to validate the derived velocities. The general workflow comprises first-break traveltime picking, construction of a simple initial model by investigating refraction branches, three-dimensional nonlinear refraction tomography and extraction of a representative two-dimensional (2D) near-surface velocity model.

Traveltime tomographic approaches often differ mainly in the ray-tracing process used for forward modelling. Furthermore the regularization applied when solving the inverse problem is another significant factor. In our workflow the inversion of traveltimes is performed using the method developed by Zhang and Toksöz (1998). They implemented a shortest path ray-tracing approach (SPR), where the minimum traveltime can be found for nodes, which are timed along the expanding wavefront. From this point on, the new wavefront is propagated and these steps are repeated until the raypaths for the whole model are calculated. Zhang and Toksöz (1998) solved the inverse problem by minimizing the misfit of the average as well as the apparent slowness. This joint minimization takes not only the traveltime but also the whole traveltime curve into account. Within the Tikhonov regularization we applied a second-order smoothing operator, which numerically leads to a cubic spline interpolation. The final objective function is linearized by the Gauss-Newton method. For solving the inverse problem the conjugate gradient technique is used.

Blötberget mining area

The study area, Blötberget, sits within the historical Bergslagen mineral district of Sweden. It is known for rich iron-oxide sometimes also apatite-bearing deposits. Down to a depth of 500 m, the deposit dips approximately 45° towards the southeast. Below this depth, the mineralized units become gently dipping until an actual known depth of 850 m from which mineralization is open to be discovered. Maries et al. (2017b) investigated physical properties from downhole logging in the Blötberget area. The mineralized zones are mainly made up of apatite-rich magnetite or hematite. Measured P-wave velocities vary around 5.0 – 6.2 km/s down to a depth of 450 m below surface, which are taken as a first constraint on the initial seismic velocity model. Constituent rocks are granites, gneissic granites as well as metamorphic volcano-sedimentary rocks.

The provided datasets for our study were acquired in 2015 and 2016 in two 2D surface reflection seismic surveys (Figure 1). The whole profile has a length of 3900 m in total and is separated by a road crossing the area from northeast to southwest. We separated the whole profile into a northern and a southern part and therefore split the datasets into three sub-datasets:

1. 2015 dataset with shooting (500-kg Bobcat drophammer, shot spacing 10 m) and recording (wireless stations, 10 m spacing) along the south-eastern part of the road,
2. 2016 dataset with shooting (500-kg Bobcat drophammer, shot spacing 5-10 m) and recording (cabled geophones with 5 m spacing and wireless stations with 10 m spacing) along the north-western part of the road,
3. 'cross-shooting' dataset with shooting (500-kg Bobcat drophammer and explosives) in the north-western part of the road and recording in the south-eastern part of the road (Figure 1, right).

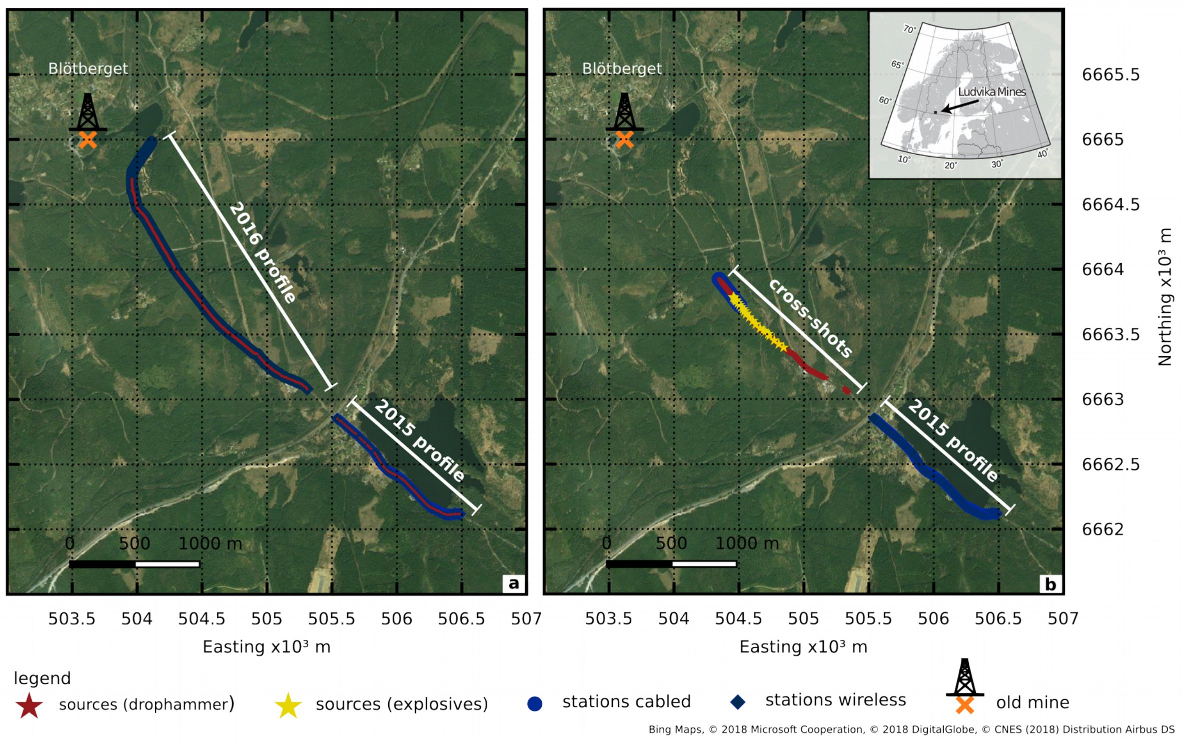

Figure 1: *Maps of the 2D seismic profiles acquired in the Blötberget mining area of Ludvika Mines in central Sweden. The profiles represent a part of the seismic surveys performed in 2015 and 2016 (Malehmir et al., 2017; Maries et al., 2017a). Seismic data used for this study consist of three sub-datasets: southern part of the 2015 profile (without landstreamer data), 2016 profile (both shown in figure **a**) and wide-angle shots (so-called 'cross-shots') with shooting in the north and recording in the south (shown in figure **b**).*

Velocity model building

An initial model is constructed by the investigation of refraction branches for the measured first arrivals of all datasets. Due to the maximum source-receiver distance (offset) of 2200 m, a maximum ray penetration depth of approximately 350 m is achieved. The initial model represents a three-layer model composed of a thin top layer representing the glacial deposits (2500 m/s), a second layer with an average velocity of 5400 m/s down to a depth of 5 m above mean sea level and a lower layer with

6200 m/s. After the inversion of the picked traveltimes including testing of different smoothing parameters, the derived velocities range from 2500 m/s to 6500 m/s.

In a second step, the tomographic model of the cross-shooting data is used as an input for the inversion of the 2015 and 2016 datasets. Due to smaller offsets of about 1200 m, a maximum ray penetration of approximately 130 m is achieved. The results show a higher resolution of the upper 100 m of the model especially in the lateral direction of the profile (Figure 2). The maximum ray coverage provides an estimate of the reliability of the different parts of the velocity model. In order to remove the remaining influence of the initial model and to keep the highly resolved parts of the model, we blended the parts of the model with no ray coverage. For a representative 2D tomographic model we included only the parts of the model with the highest ray coverage (Figure 2).

The derived velocity models are characterized by a thin weathering layer with minimum velocities around 2500 m/s and a strong vertical velocity gradient. For a crystalline environment strong velocity gradients are known for the upper several hundred meters which can also be observed in the presented results. In particular for the middle part of the 2015 profile a strong increase of the P-wave velocity up to 5500 m/s – 6000 m/s indicates that the host rock already occurs at a depth of approximately 25 m below the surface.

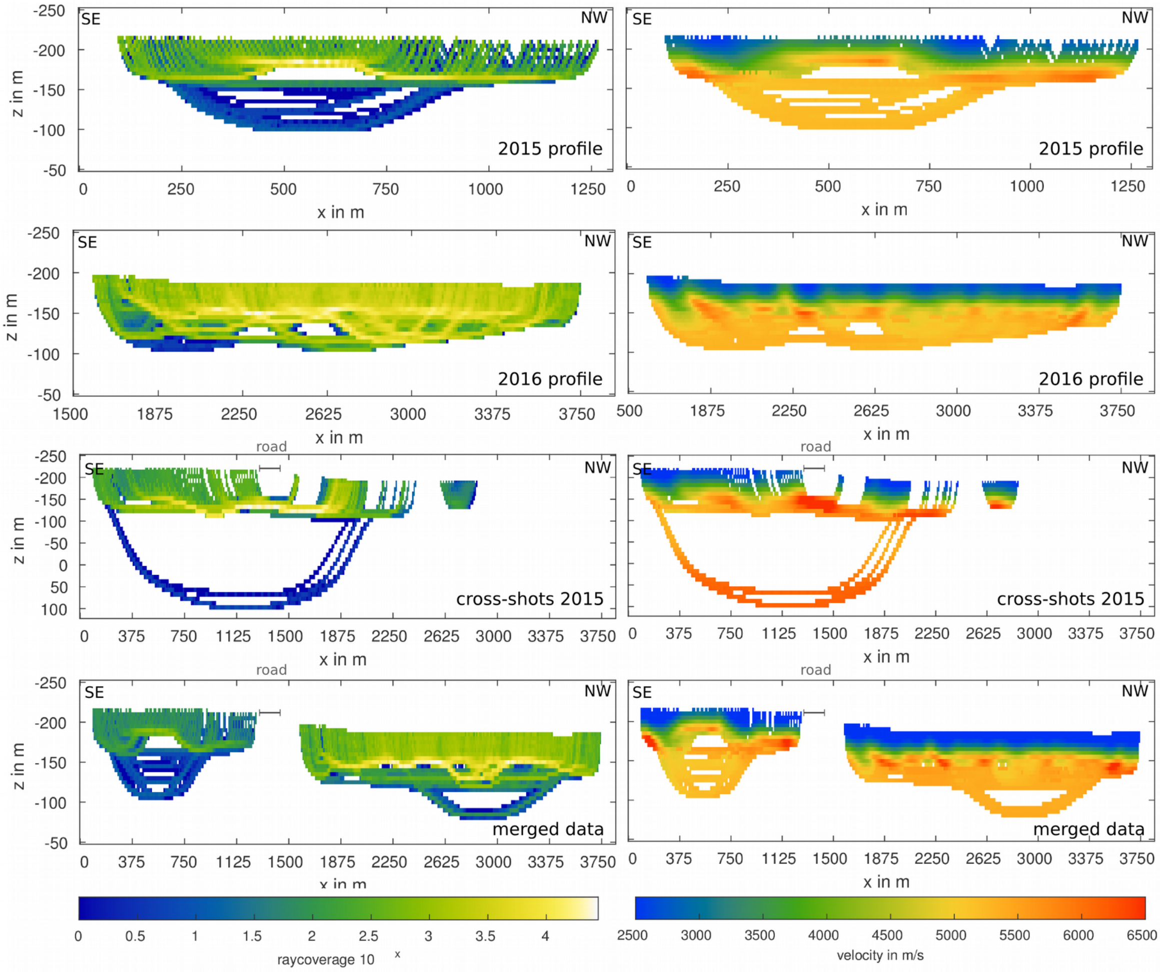

Figure 2: *Results of the first-break traveltime tomography for the three different sub datasets. Left: projected ray coverage. Model parts without ray penetration are omitted. Right: representative two-dimensional projection of the tomographic model showing velocities between 2500 m/s and 6500 m/s. The inversion result of the cross-shooting dataset is used as initial velocity model for the inversion of the traveltimes of the 2015 and 2016 dataset. The depth axis is in meters below mean sea level.*

The resolution of the tomographic models is calculated for an apparent velocity of 5000 m/s and a maximum propagation distance of 350 m. Assuming a dominant frequency of the first arrivals of 50 Hz, a minimum wavelength of 100 m can be estimated. Therefore the width of the first Fresnel zone, which represents the lateral resolution, can be estimated to about 265 m. The vertical resolution can be estimated by the quarter-wavelength criterion and is about 25 m. Geological features smaller than that width or thickness, respectively, cannot be resolved. Taking into account the average propagation distance of 130 m, the width of the first Fresnel zone reduces to 160 m. Comparing the synthetic first arrival times calculated for the final tomographic model with the picked first arrival times, a very good fit of the traveltimes can be observed with a maximum misfit on the order of 3-7 ms.

Conclusions

Within the Smart Exploration project, existing seismic data acquired in the Blötberget mining area have been used for a delineation of deposits at depth. Advanced seismic depth imaging methods will be used to reveal a clear image of the subsurface. A successful positioning of the reflectors as well as focusing of the seismic energy at the reflector's position requires a reliable and well-resolved migration velocity model in order to compensate for energy losses and wavefield scattering effects due to the heterogeneity of the crystalline environment, strong lateral inhomogeneities of the glacial cover as well as strong topographic effects on the seismic wavefield. The application of first-break traveltime tomography yields a near-surface velocity model with high resolution and velocities ranging between 2500 m/s and 6500 m/s. The derived velocities are in the range of literature values for granite and gneiss from that area and indicate a strong velocity gradient for the first several hundred meters. Especially for the southern part of the profile the host rock occurs at a shallow depth of approximately 25 m below the surface. The average velocity of the host rock varies between 5500 m/s and 6000 m/s. Such a tomographic model can directly be incorporated into a robust migration velocity model and therefore acts as a basis for an iterative velocity analysis in the later prestack depth migration process in order to update the velocity at the reflectors.

Acknowledgements

We thank Uppsala University and Nordic Iron Ore AB (NIO) for providing access to the raw shot records and collaborating with us through the Smart Exploration project. Smart Exploration has received funding from the European Union's Horizon 2020 research and innovation program under grant agreement No. 775971.

References

Buske, S., Gutjahr, S., Sick, C. [2009] Fresnel volume migration of single-component seismic data. Geophysics, 74, WCA47–WCA55, 10.1190/1.3223187.

Hlousek, F., Hellwig, O., Buske, S. [2015] Improved structural characterization of the Earth's crust at the German Continental Deep Drilling Site using advanced seismic imaging techniques. Journal of Geophysical Research, Solid Earth, 120, 6943–6959.

Malehmir, A., Maries, G., Bäckström, E., Schön, M., Marsden, P. [2017] Developing cost-effective seismic mineral exploration methods using a landstreamer and a drophammer. Scientific Reports, 7, 1.

Maries, G., Malehmir, A., Bäckström, E., Schön, M., Marsden, P. [2017a] Reflection seismic imaging of iron-oxide deposits: an example from Bergslagen mining district of Sweden. Near Surface Geoscience, Malmö-Sweden, September 2017.

Maries, G., Malehmir, A., Bäckström, E., Schön, M., Marsden, P. [2017b] Downhole physical property logging for iron-oxide exploration, rock quality, and mining: An example from central Sweden. Ore Geology Review, 90, 1–13.

Zhang, J., Toksöz, M. N. [1998] Nonlinear refraction traveltime tomography. Geophysics, 63(5), 1726–1737.